Simulation of operational conditions of HX-HERO in the CIRCE facility with CFD/STH coupled codes

F. Galleni[a,*], G. Barone[a], D. Martelli[b], A. Pucciarelli[a], P. Lorusso[c], M. Tarantino[b], N. Forgione[a]

[a] Dipartimento di Ingegneria Civile e Industriale, Università di Pisa, L.go Lucio Lazzarino n. 2, Pisa, Italy
[b] ENEA, Cento Ricerche Brasimone, Località Brasimone, Camugnano, BO, Italy
[c] DIAEE, Nuclear Section, "Sapienza" Università di Roma, 00186 Roma, Italy

ABSTRACT

The paper describes the application of a coupled methodology between Fluent CFD code and RELAP5 System Thermal-Hydraulic code developed at the DICI (Dipartimento di Ingegneria Civile e Industriale) of the University of Pisa. The methodology was applied specifically to the LBE-water heat exchanger HERO located inside the S100 vessel of the CIRCE facility, built at ENEA Brasimone Research Centre, to investigate the capabilities of this component. In the proposed methodology, the primary side of the HX-HERO, containing LBE, is simulated by the CFD code, while the secondary side, containing a two phase mixture of water and vapour, is reproduced by the System Thermal-Hydraulic code. During the calculation the two codes exchange, at the coupled boundaries: the bulk temperature and heat transfer coefficient of the ascending water (RELAP5 to Fluent) and the wall temperature at the water side surface of the pipes (Fluent to RELAP5). The coupling technique was tested by comparing the numerical results with the experimental data recently obtained by ENEA; the numerical results predicted well the qualitative trend of the temperature and provided an overall good prediction of the temperature also from a quantitative point of view. It is worth noticing that this good performance remained reliable for all the cases simulated, proving the general applicability of the methodology.

1. Introduction

System Thermal-Hydraulic codes (STH) are extensively used to provide support to the design and licensing of the thermal-hydraulic systems of Nuclear Power Plants (NPPs), e.g. RELAP5, CATHARE, TRACE, etc., are some examples of the existing codes available for this purpose. In particular, these STH codes are essential for nuclear safety analysis, since they provide good estimates of transients and postulated accidental scenarios evolutions in NPPs.

STH codes are commonly based on the one-dimensional form of mass, momentum and energy balance equations for two phase flows and they include equations of state for each fluid and empirical correlations to model the interaction between the phases (e.g. heat transfer, frictional pressure losses, etc.). Presently, their development has reached a high standard of accuracy which permits the prediction of NPP behaviours within acceptable computational time.

Nevertheless, the STH codes are not appropriate for the application to the analysis of complex three-dimensional problems such as, for instance, mixing and thermal stratification in large pool systems. On the other hand, over the last years the application of Computational Fluid Dynamics (CFD) to the Nuclear Reactor Safety (NRS) field has widened. The possibility to obtain a fine discretization of the domains allows to simulate phenomena characterised by smaller scales. Furthermore, the implementation of models - significantly closer to reality than those used in STH codes - to simulate different phenomena such as turbulence, heat transfer and chemical reactions, has made these codes sufficiently reliable for single phase flows, even in the study of complex 3D phenomena. However, considerably higher computational efforts are necessary than those required by STH codes.

In this situation, it is understandable the high interest in the development of advanced coupling techniques between STH and CFD codes for thermal-hydraulic analysis. These techniques allow to achieve a precise and affordable solution to predict the behaviour of NPP components, since the coupling methodology allows to achieve a level of detail spanning several scales. The STH codes should be used to model 1D systems (e.g., pipe) and to simulate multiphase flow in regions where 3-D phenomena are not relevant, whereas the CFD codes should analyse parts of the domain where 3D effects are not negligible or extensive flow information is required.

In this frame, the University of Pisa developed an in-house coupling

---

* Corresponding author.
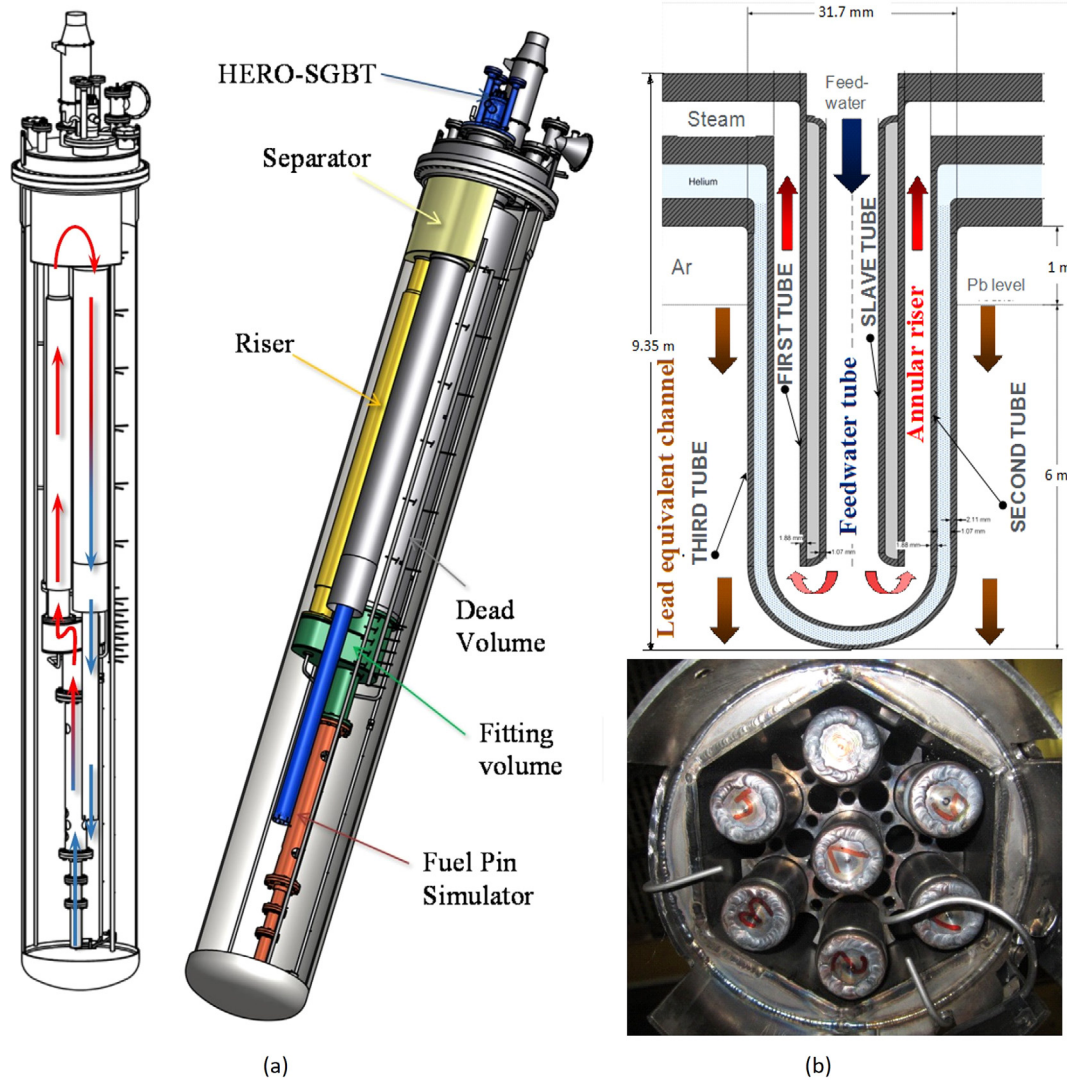 E-mail address: francescog.galleni@dici.unipi.it (F. Galleni).

Fig. 1. CIRCE-HERO facility: test section (a) and HERO heat exchanger bayonet tube (b).

Table 1
CIRCE S100 vessel main parameters.

Parameter	Value
Outside Diameter	1200 mm
Wall Thickness	15 mm
Material	AISI 316L
Max LBE Inventory	90000 kg
Electrical Heating	47 kW
Cooling Air Flow Rate	3 Nm³/s
Temperature Range	200–550 °C
Operating Pressure	15 kPa (gauge)
Design Pressure	450 kPa (gauge)
Argon Flow Rate	0–15 Nl/s
Argon Injection Pressure	600 kPa (gauge)

Table 2
HERO SGBT tubes design.

Label	Outer Diameter [mm]	Thickness [mm]	Material
Slave Tube	9.53	1.22	AISI 304
First Tube	19.05	1.65	AISI 304
Second Tube	25.40	2.11	AISI 304
Third Tube	33.40	3.38	AISI 304

methodology between the Ansys Fluent CFD code (ANSYS Inc., 2018) and RELAP5/Mod3.3 STH code (Nuclear Safety Analysis Division, 2001). Specifically, the coupling technique was used to simulate the NACIE (NAtural CIrculation Experiment) experimental loop and the CIRCE (CIRColazione Eutettico) experimental pool (Angelucci et al., 2017a,b; Martelli et al., 2017a; Forgione et al., 2019). These activities were carried out in association with the Research Center of ENEA at Brasimone (Italy), where the facilities were designed and constructed. In the present work, the coupling method was applied to the HERO

(Heavy liquid mEtal pRessurized water cOoled tubes) heat exchanger installed in the CIRCE facility (see Fig. 1). The CIRCE-HERO facility was created in the context of the SESAME H2020 project (Simulations and Experiments for the Safety Assessment of Metal cooled reactors) and then modified to suit the needs of the H2020 project MYRTE (MYRRHA Research and Transmutation Endeavour). The MYRTE project focused on the development of the MYRRHA reactor (Multi-Purpose Hybrid Research Reactor for High-Tech Applications), in support of MYRRHA design and pre-licensing (Baeten, 2015; MYRTE Project, 2015; Roelofs et al., 2015). More specifically, the experimental campaign conducted on the CIRCE-HERO facility was mainly dedicated on the understanding of the influence of several parameters on the heat removal capabilities in steady state conditions of the Primary Heat eXchanger (PHX) designed for the MYRRHA reactor (Lorusso et al., 2019a).

Table 3
CIRCE HERO Experimental campaign of 2018 – Test matrix of operative conditions.

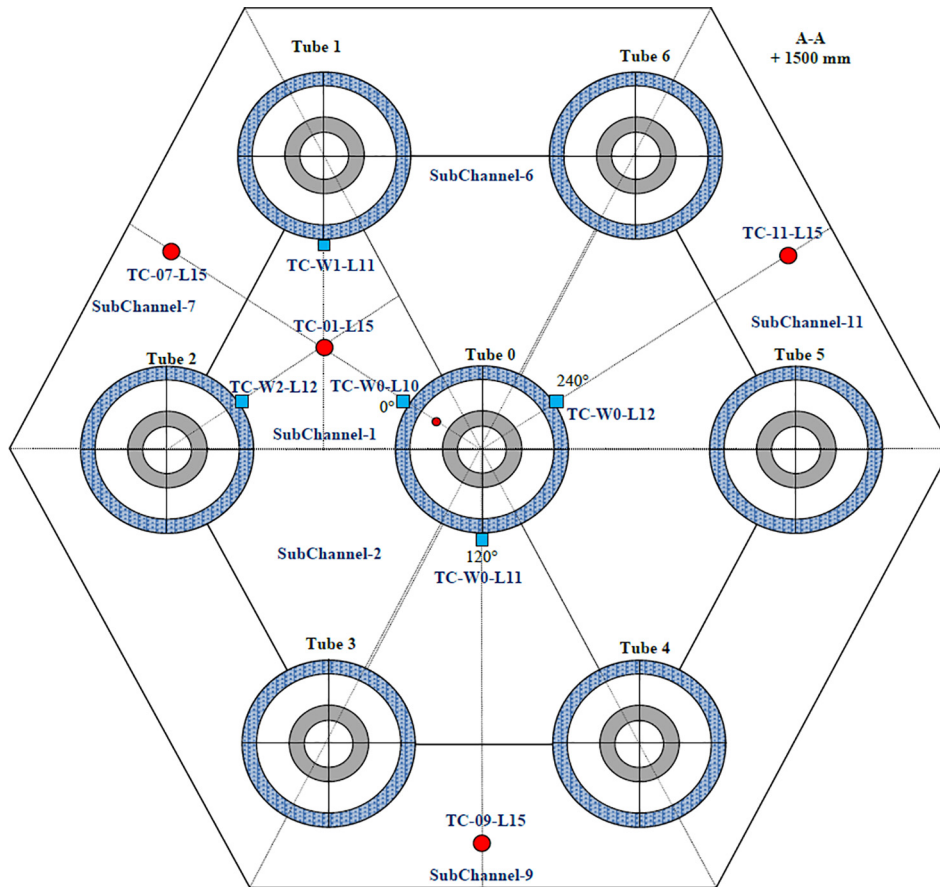| Parameter	Test 0	Test 1	Test 2	Test 3	Test 4	Test 5	Test 6	Test 7	Test 8
LBE mass flow [kg/s]	30	31	31	*39*	*20*	30	31	30	30
LBE inlet temperature [°C]	238	*258*	*213*	236	244	236	236	239	239
Water mass flow rate [kg/s]	0.16	0.16	0.16	0.16	0.16	0.16	0.16	*0.218*	*0.12*
Water inlet temperature [°C]	200	198	198	198	198	*218*	*178*	199	198
Secondary outlet pressure [bar]	16	16	16	16	16	*23*	16	16	16

Fig. 2. Thermocouples radial positions in the HERO test section (Pesetti et al., 2018).

2. CIRCE – HERO facility

2.1. Test-section description

The CIRCE facility (Fig. 1) is an integral effect pool type facility using Lead-Bismuth Eutectic (LBE) as primary coolant, dedicated to the study of innovative nuclear systems cooled by liquid heavy metal (Ambrosini et al., 2004; Benamati et al., 2007; Martelli et al., 2017b; Narcisi et al., 2017). It consists of a main vessel S100, in which the HERO test section is installed. A detailed description of the facility can be found in Lorusso et al., 2018. The main parameters are reported in Table 1.

The primary side consists of the following components:

- Fuel Pin Simulator (FPS), electrically heated, which provides a nominal thermal power of ~1 MW;
- Fitting volume, in which the LBE coming from the FPS is collected;
- Riser, through which the LBE flows from the fitting volume up to the separator;
- Separator, that is situated at the top of the test section and acts as a hot plenum.

- Steam Generator Bayonet Tube;
- Argon gas-lift pump device, placed at the bottom of the riser.

The LBE mass flow rate in the CIRCE-HERO facility under gas-enhanced circulation conditions is obtained by setting a proper argon flow rate injected at the bottom of the riser tube in order to generate the driving force of a pumping system.

In the separator the argon gas is then separated from the LBE and recirculated from the cover gas outside the main vessel in the argon loop to maintain the pressure in the cover gas almost constant.

As for the secondary side, the HERO Steam Generator Bayonet Tube (SGBT), shown in Fig. 1(b), consists of seven double-walls bayonet tubes arranged in a hexagonal shroud (the bayonet tube dimensions are summarized in Table 2) with stainless steel powder filling the gap and with intermediate leakage monitoring; spacer grids contribute in maintaining the correct tubes positioning along the axial direction The secondary circuit of the HERO Heat Exchanger (HX-HERO) is fed by pressurized, pre-heated, water; the pre-heater has maximum heating power of 500 kW.

The feedwater enters the unit at the top edge of the slave tube, it flows downward and it is collected into the lower plenum. Then water
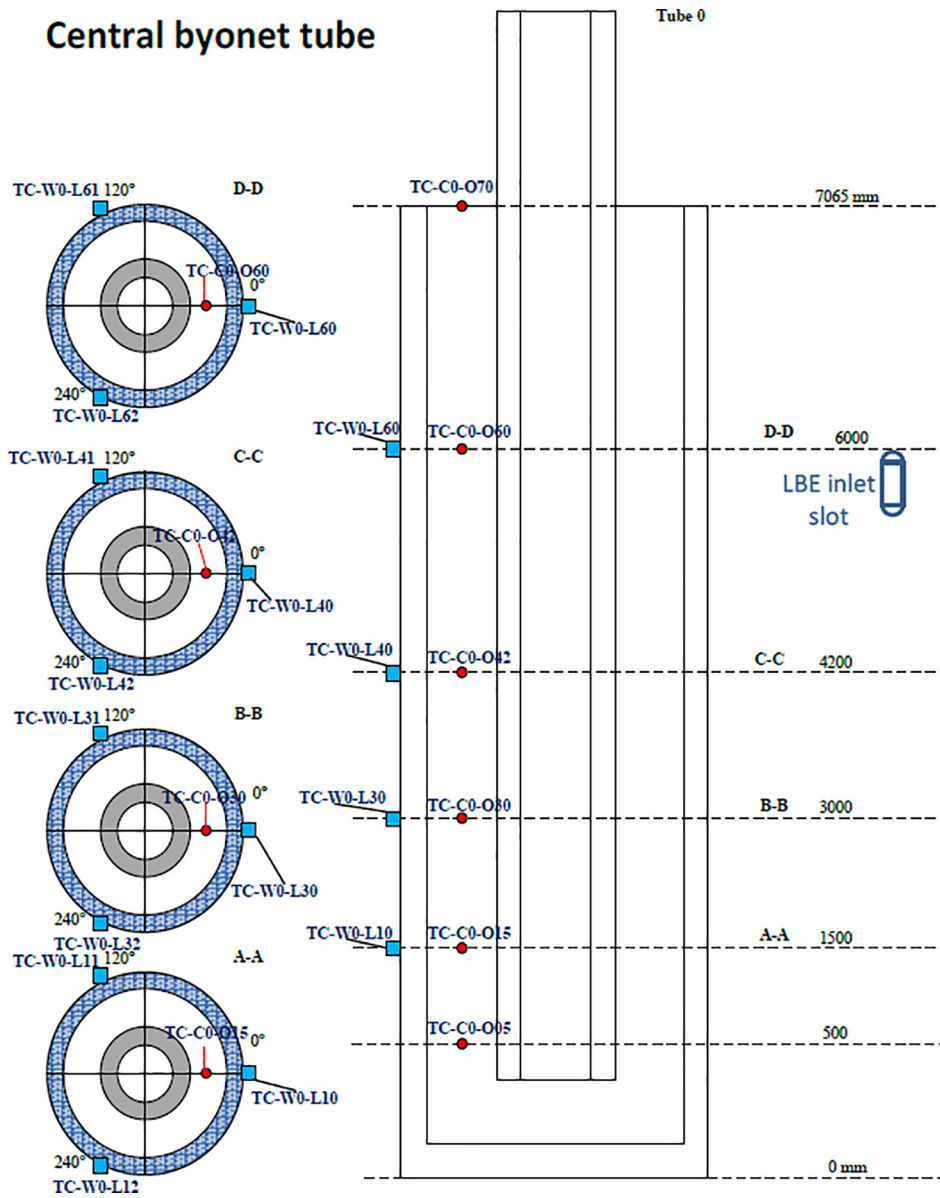
Fig. 3. Thermocouples axial positions in the HERO test section (Pesetti et al., 2018).

flows upward through the annular riser between the first and second tube and the steam is collected into the steam chamber.

The gap between slave and first tube is filled with air (slight vacuum) acting as insulator to avoid steam condensation. The gap between second and third tube is filled with AISI316L powder and slightly pressurized helium (~10 bar) to detect any leakages, monitoring helium pressure, and while maintaining a good heat exchange capability thanks to the metallic powder. The ends of the bayonet tubes are closed with a welded steel cap.

2.2. Experimental campaign

In the experimental campaign conducted at ENEA Brasimone Research Centre in the framework of the HORIZON2020 MYRTE European project – a test reference was chosen (TEST 0), and, starting from the obtained steady state conditions, a sensitivity analysis was conducted by changing one parameter at a time. In total 9 experimental tests were performed: the main parameters are summarised in Table 3, with the parameter changed with respect to the reference test in bold and italic; furthermore, an extensive presentation of the experimental

results can be found in the technical report by Lorusso et al. (2018).

2.3. Instrumentation

The test section of the CIRCE-HERO facility includes several instrumentation tools to measure the parameters which characterise each experiment. In the next sections only the instrumentation which is relevant to the present work will be described. Further details can be found in Lorusso et al. (2019a,b).

On the shell side of the Steam Generator 18 TCs measure the LBE temperature at the inlet, outlet and at three different axial positions of the steam generator. Other 18 TCs acquire the outer wall temperature (LBE side) along the central BT and two external BTs.

The instrumentation in the secondary loop (i.e. water side) is composed of 12 thermocouples, 9 relative and 4 differential pressure transmitters. Specifically, the annular rising part of the central BT is instrumented with 5 TCs, disposed at five different axial positions. Furthermore, 1 TC is placed on the upper part of each BT, in order to measure the outlet steam temperature. The axial and azimuthal positions of the TCs of the central bayonet tube (with the zero placed at the
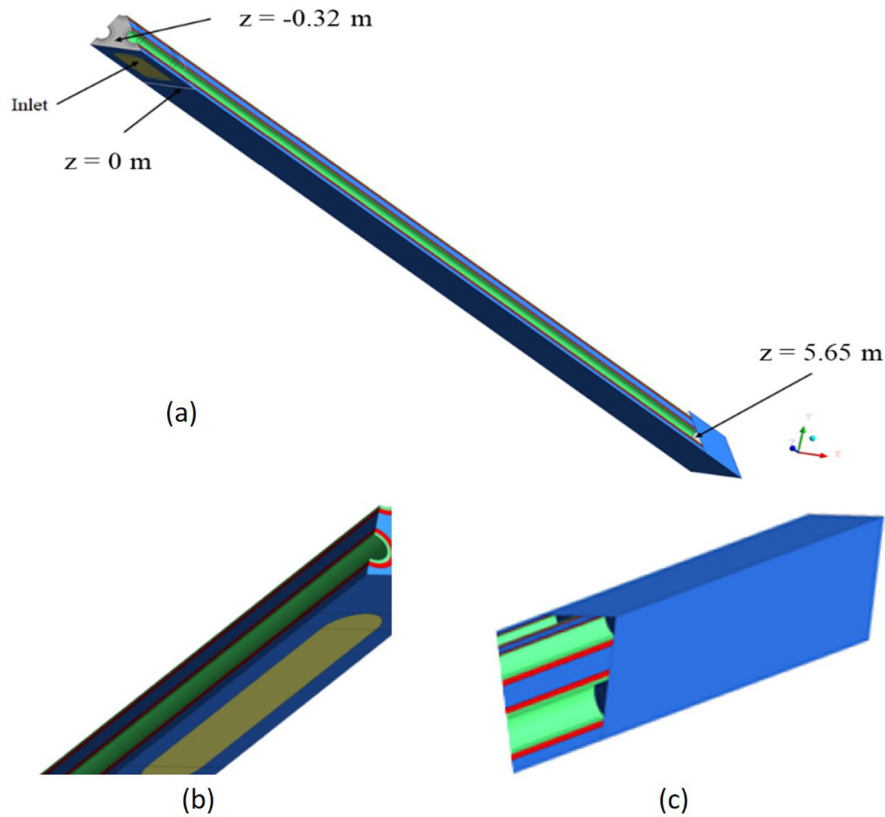
Fig. 4. HERO periodic geometrical domain: overall geometry (a), LBE inlet (b) and outlet (c) region.
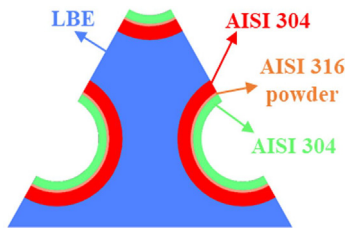

Fig. 5. HX-HERO fluid and solid regions.

bottom of the SGBTs), can be found in Fig. 2 and Fig. 3.

It is important to notice that not all the probes described above were actually working during the experimental campaign; for instance, the data from all the probes denominated TC-W0-L6# in Fig. 3 were not provided. In the comparison between the simulations and the experimental data presented in the following sections all the available measurements were used.

3. Coupled simulations

3.1. CFD model assessment

A CFD three-dimensional model of the primary side of HX-HERO was created, comprising the solid structures and the LBE domain; the mesh was generated using the ANSYS Workbench tool (ANSYS Inc., 2018). Given the symmetry of the test section, only one sixth of the whole geometry was simulated. This simplification decreased the number of cells of the spatial discretization and therefore reduced the computational time. Fig. 4(a) shows the geometry used in the CFD calculations, whereas the details of the inlet and outlet regions are shown respectively in Fig. 4(b) and Fig. 4(c). The yellow region in Fig. 4 (a-b) represents the LBE lateral inlet section and it replicated one of the six entrance slots in the HX-HERO test section.

Fig. 5 presents the cross section with the different regions reproduced in the CFD model: the LBE zone is shown in blue, whilst the solid parts made of AISI 304 steel are represented in red (in contact with the LBE side) and green (in contact with the water side). The thin orange zone in between the two steel pipes regions is the AISI 316 powder.

The spacer grids supporting at regular axial intervals the bayonet tubes were not represented in the CFD domain; nevertheless, their impact on the flow is usually local. As a consequence, by neglecting the spacer, the computational cost of the simulations is relevantly reduced without impairing the quality of the obtained predictions.

The thermodynamic properties of the LBE (i.e. density, molecular viscosity, thermal conductivity and specific heat) were implemented in the CFD code as polynomial functions of the temperature in agreement with OECD/NEA Handbook (Fazio et al., 2015).

It is worth noticing that the properties chosen for the AISI 316 powder were uncertain to some extent; however, since the simulations performed were all steady state, the density and specific heat did not affect the results. As for the thermal conductivity, it would usually depend on the temperature; however, a constant value was chosen for the sake of simplicity as first attempt. In the addressed experimental cases, temperatures in the range of 230–260 °C were observed in the HERO SGBT; as a consequence, a thermal conductivity value of 3.3 W/mK was selected in accordance with the thermal properties tables provided by the designers (Pesetti et al., 2018). Calculations assuming thermal conductivity which depended on the temperature were performed as well, reporting a negligible impact on the obtained results for the considered cases.

All the calculations were performed adopting the Realizable k-ε model together with standard wall functions for the simulation of the near wall region. Liquid metals report a molecular Prandtl number in range of 0.01 making the Reynolds analogy hardly applicable to heat transfer problems involving these fluids. Though this problem may require the use of advanced modelling techniques (Shams et al., 2014), in
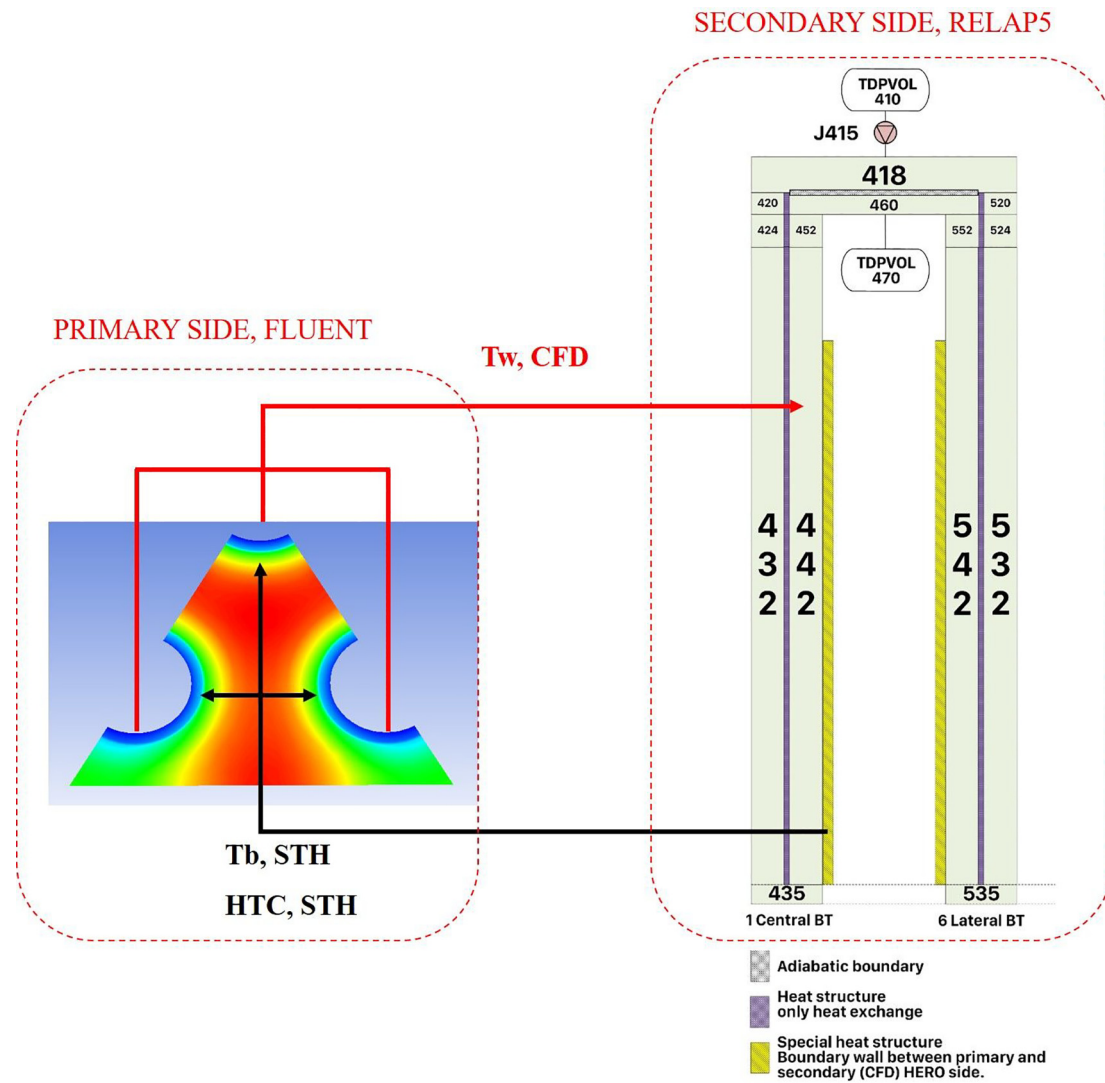
Fig. 6. HERO tubes RELAP5 nodalization and variables exchanged through the interfaces.
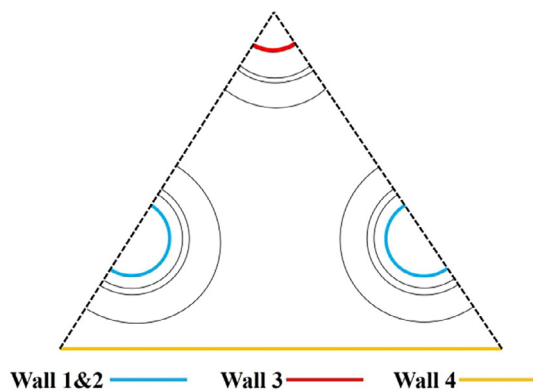

Fig. 7. CFD domain walls location.

literature it is often overcome by simply assuming a turbulent Prandtl number in the range 1.5–3.0. This technique proved interesting predicting capabilities suggesting that a good modelling may be obtained even with such a simple approach. In similarity with other works performed at the University of Pisa (Buzzi et al., 2020; Pucciarelli et al., 2020), a turbulent Prandtl number equal to 1.5 was set for all the performed calculations.

Eventually, concerning the boundary conditions, mass flow inlet and pressure outlet conditions were considered; symmetry conditions were also assumed in accordance with the postulated characteristics of the considered domain. A convective condition was instead imposed on the internal side of the bayonet tubes in order to simulate heat transfer with the two-phase water flowing in the steam generator. Particularly, these surfaces also represent a coupling interface between the CFD and the STH code; during the coupled calculation, the required values for the convective heat transfer coefficient and the environmental temperature are thus provided by the STH code at each simulation.

3.2. RELAP5/Fluent coupling procedure

A coupled model of the HERO test section was developed in order to analyse comprehensively the performances of this component. The HX primary side and the heat structure were simulated by the CFD code, whilst the secondary side, containing water-vapour, was modelled with the STH code RELAP5. The methodology can be defined as "non-overlapping", because the regions modelled with the CFD code are not modelled with RELAP5 and vice versa.

The scheme adopted for the thermal coupling and the variables exchanged through the interfaces of the two domains are shown in Fig. 6.

As it can be observed, the RELAP5 domain consists in a simple nodalization representing the secondary side of the CIRCE-HERO
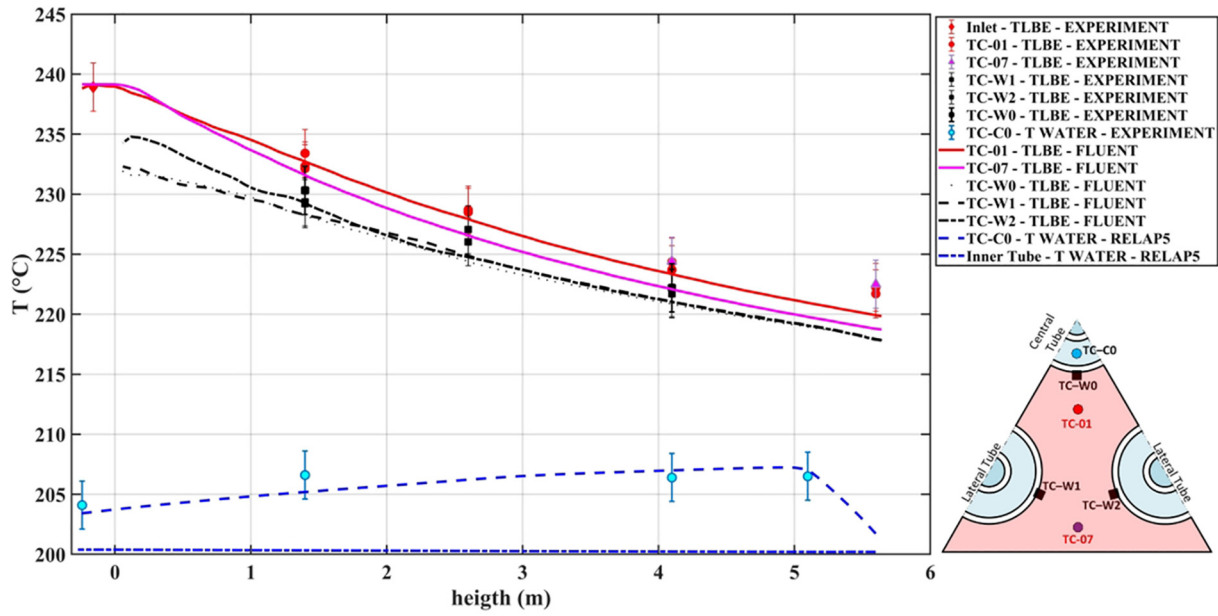
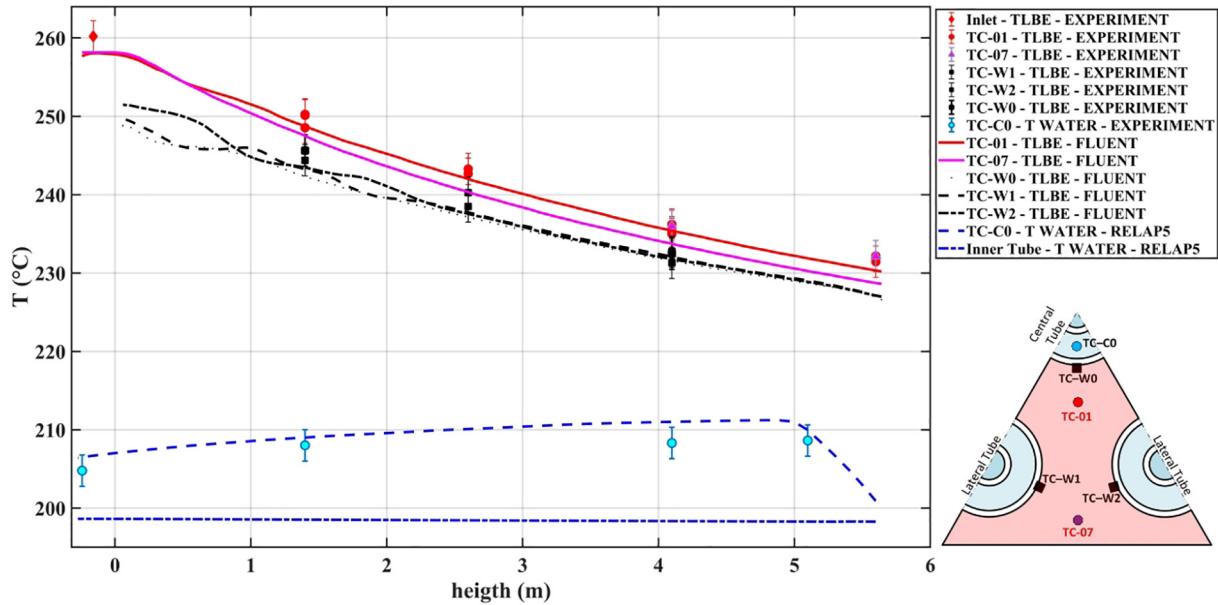**Fig. 8.** Coupled simulations – Temperature axial evolution in Test 0.

Fig. 9. Coupled simulations – Temperature axial evolution in Test 1.

facility. The central bayonet tube is simulated by a dedicated pipe (pipe from 420 to 452); the six external tubes are instead simulated together (pipe from 520 to 542), assuming suitable values for the hydraulic diameter and the heat transfer interfaces. This design is related to the assumption that the temperature distributions on the external tubes can be considered equals because of symmetry reasons; a different distribution is instead to be expected for the central tube which is coherently simulated alone. The HERO SGBT inlet conditions are imposed through the TDV 410 where temperature and pressure are imposed and the TDJ 415 which instead assigns the mass flow rate. Concerning the thermal boundary conditions, the temperature is imposed on the external side of the heat structures connected to pipes 442 and 542 which also represent the RELAP5 side coupling interface between the CFD and the STH code.

In the adopted coupling scheme, at each step, the following variables are exchanged:

- Water/two phase mixture bulk temperatures (Tb);
- Heat Transfer Coefficient (HTC) at the wall of the pipes of the ascending water/two-phase mixture;
- Steam side wall temperature (Tw) of the ascending bayonet tube.

The variables were exchanged at the walls of the ascending water pipes (walls 1, 2 and 3 in Fig. 7) and, coherently with the adopted RELAP5 nodalization, the data were distinguished between the central and the lateral pipes. By exchanging these values, both the CFD and STH domains are provided with well-defined boundary conditions; an additional check on the calculated heat fluxes is also performed in order to assure the conservation of energy across the coupling interface.

In order to achieve a better representation of the axial temperature trends inside the steam generator, the RELAP5 components pipe 442 and pipe 542, representing the ascending part of the bayonet tubes, were subdivided, axially, into 60 subvolumes. Each subvolume is
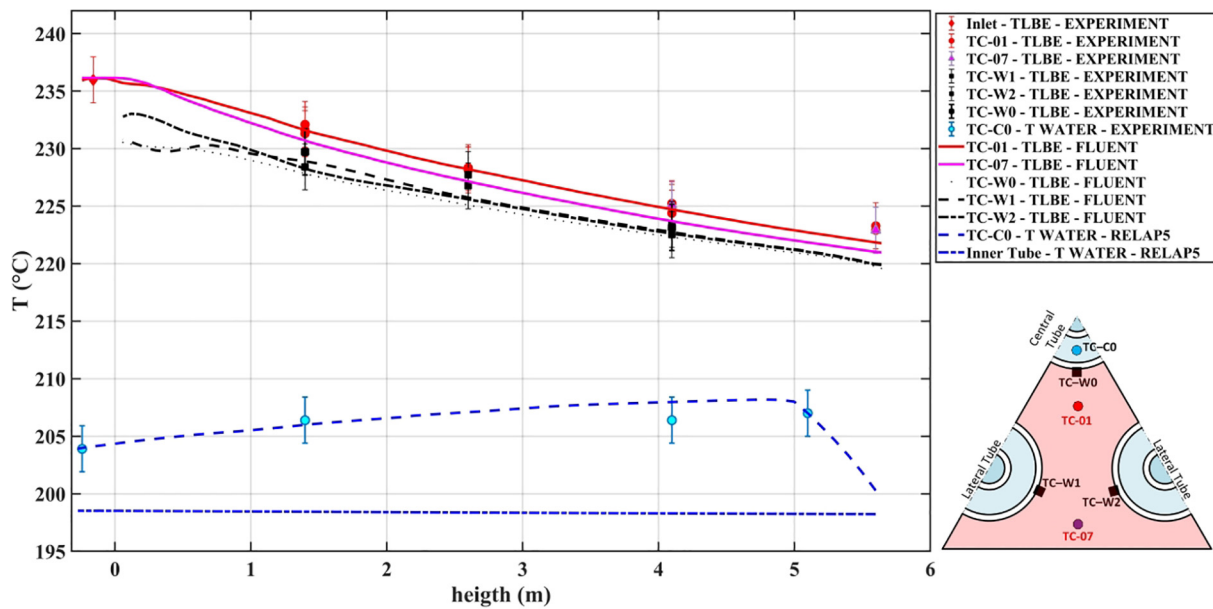
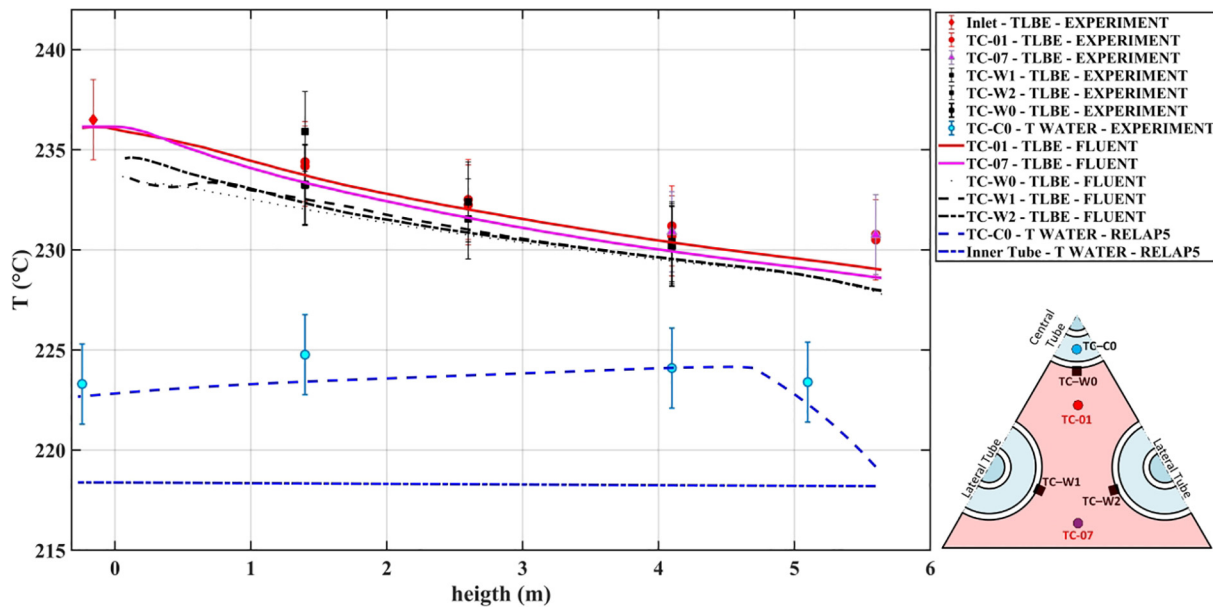**Fig. 10.** Coupled simulations – Temperature axial evolution in Test 3.

Fig. 11. Coupled simulations – Temperature axial evolution in Test 5.

equipped with a dedicated interface with the CFD side providing the required boundary conditions. As a consequence, 60 axial subdivision of each boundary wall of the CFD domain were generated. Actually, the surfaces were created on Wall 2 and Wall 3, since the division of Wall 1 was not needed because of the symmetry.

At every iteration, firstly CFD performs a calculation basing on the boundary and initial conditions calculated at the previous iteration. After, the wall temperatures calculated by the CFD code are averaged over the surface of the pipes in each of the 60 axial interface zones; then these data were transferred to the corresponding surfaces on the RELAP5 side. Consecutively, RELAP5 performs its calculation adopting the updated boundary conditions and providing 60 data points of the two-phase water mixture bulk temperature and the HTC, from which an axial profile was built (with a linear trend). These temperature and HTC profiles are then provided back to CFD code as boundary conditions that will be used during the following iteration.

Being the addressed operating conditions at the steady state, the

coupling strategy was to perform RELAP5 calculations of very long transient (2000 s) assuring the achievement of steady state conditions; on the CFD side, instead, steady state calculations were performed. The chosen criteria for iteration convergence was the relative difference between the values of each variable at two consecutive iterations. The convergence criterium for exchanged temperatures was a relative difference lower than 1%; a weaker criterion, requiring differences lower than 10%, was instead considered for the heat transfer coefficient owing to the intrinsic difficulties in simulating heat transfer involving a two-phase mixture. In addition, after each iteration, the heat transferred at the coupling interfaces of each domain is calculated, in order to check the conservation of energy before proceeding to the following time level. Further information on the coupling algorithm can be retrieved in Angelucci et al. (2017a) and Forgione et al. (2019).
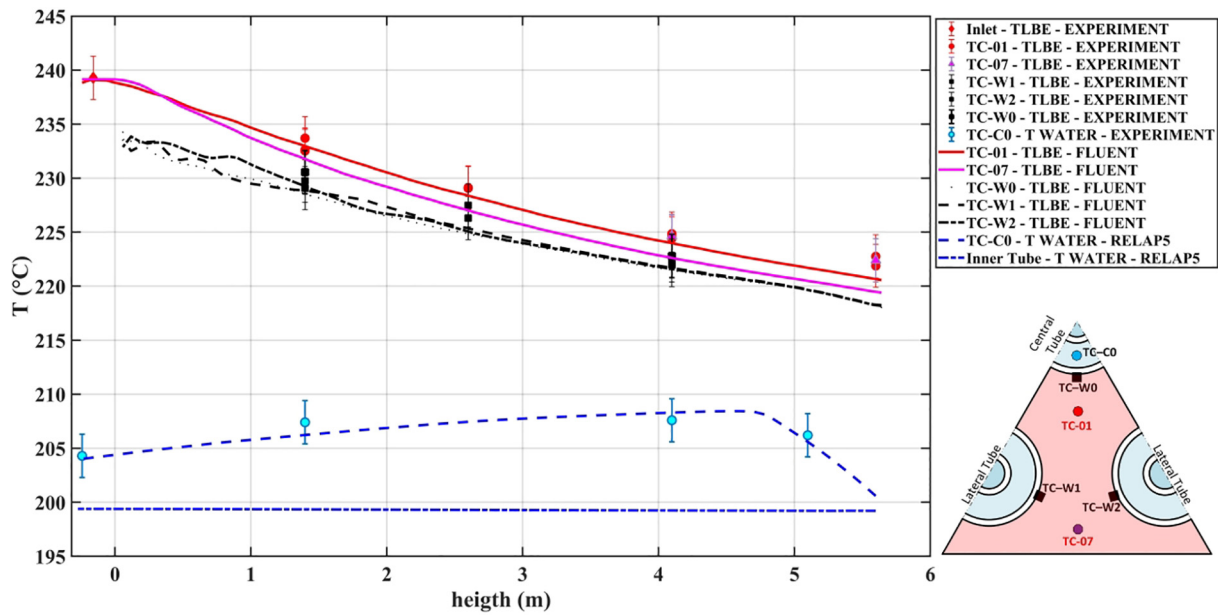
Fig. 12. Coupled simulations – Temperature axial evolution in Test 7.
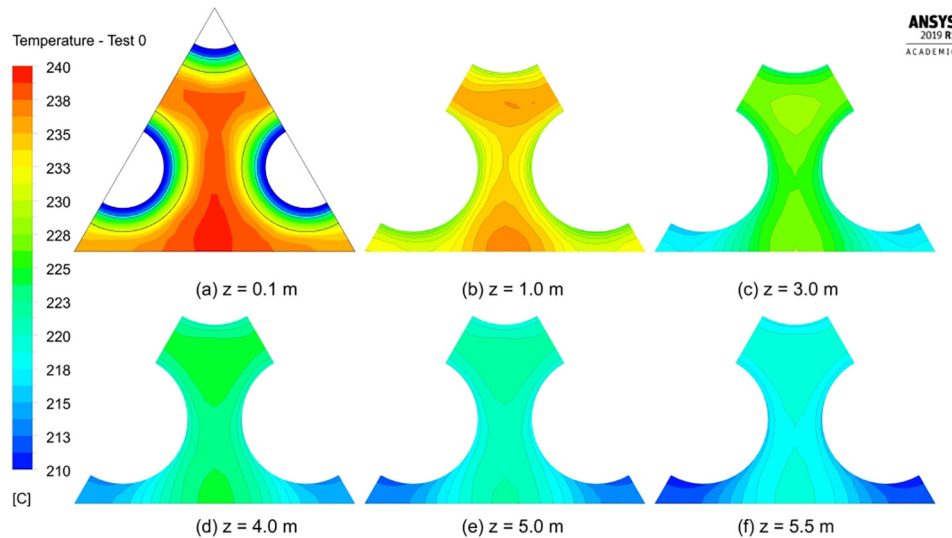

Fig. 13. Coupled simulations – Temperature distribution at different heights in Test 0.

4. Obtained results

As described in section, 9 experimental test were simulated using the coupled domain between Fluent and RELAP5. The most representative numerical results are presented from Figs. 8–17 and compared with the experimental data of 5 tests; these 5 cases were chosen since they refer to the very different operating conditions spanning from the minimum to the maximum mass flow rates and providing also a good sample of the effects of the variation of the imposed water inlet temperature. As a general comment of the proposed figures, it can be observed that the considered operating conditions seem not to impact relevantly on the obtained results. This suggests that the investigated steam generator seems able to filter potential fluctuations of the operating conditions without undergoing relevant efficiency impairments.

In all the figures, the lines (continuous or dashed) represent the results obtained through the simulations, whilst the dots represent the experimental data; an absolute measuring error of ± 2 °C is also added to the experimental data (Pesetti et al., 2018).

The temperatures are compared for the primary and secondary sides (i.e. LBE and water/vapour, respectively) at different axial and angular positions.

4.1. Temperature – axial profile

Regarding the axial profile of the temperature, all the simulations show the same behaviour. In the secondary side, the temperature of the liquid water – flowing downward – remains approximately constant for the whole length of the pipe; on the vapour side (i.e., the annulus) the water evaporates while it flows upward. Since the fluid is in saturated conditions, the temperature slightly decreases in accordance with the pressure decreasing connected with the distributed pressure drops. This trend is well captured by the coupled simulation, both qualitatively and quantitatively, with all the predictions staying inside the measurement error.

On the LBE side, although the trend is again well captured, the axial temperature of the liquid metal is slightly under-predicted. However, the error due to this under-prediction remains small; the maximum
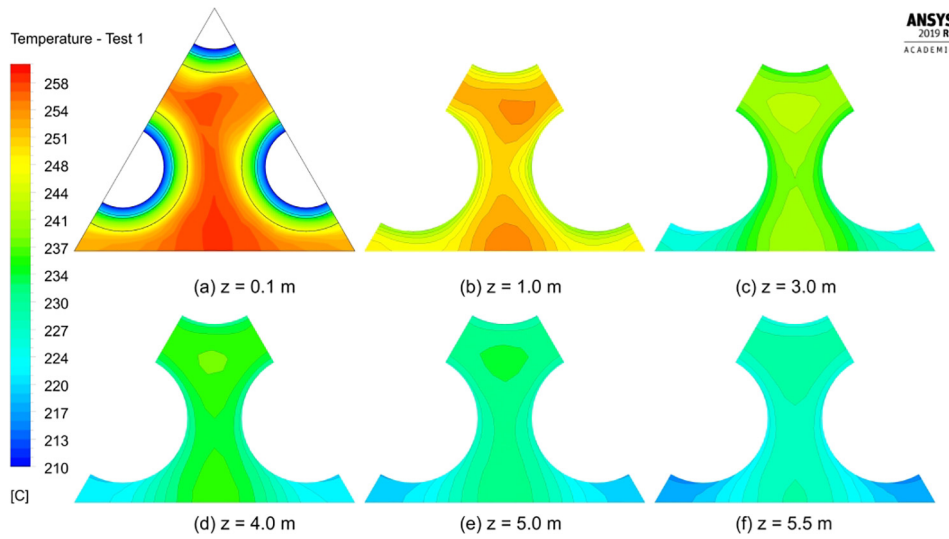
F. Galleni, et al.

Fig. 14. Coupled simulations – Temperature distribution at different heights in Test 1.
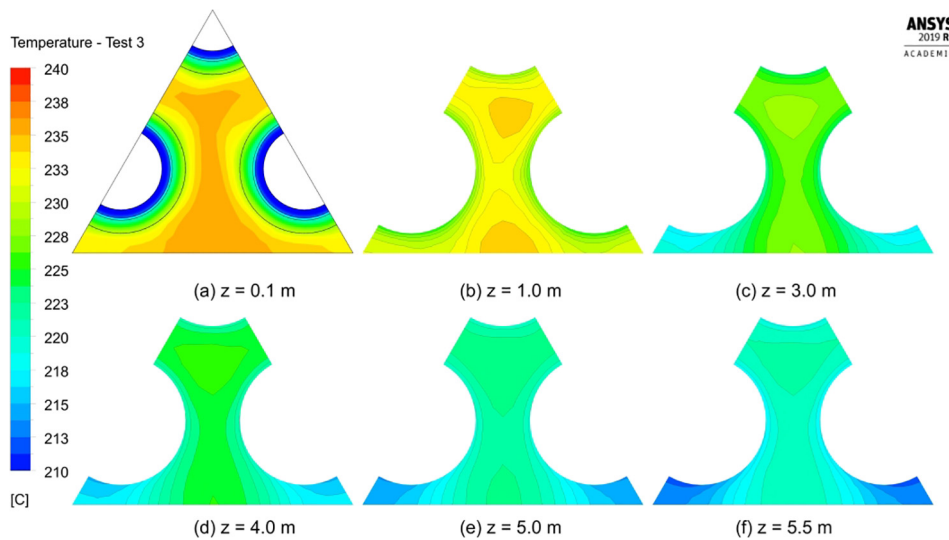

Fig. 15. Coupled simulations – Temperature distribution at different heights in Test 3.
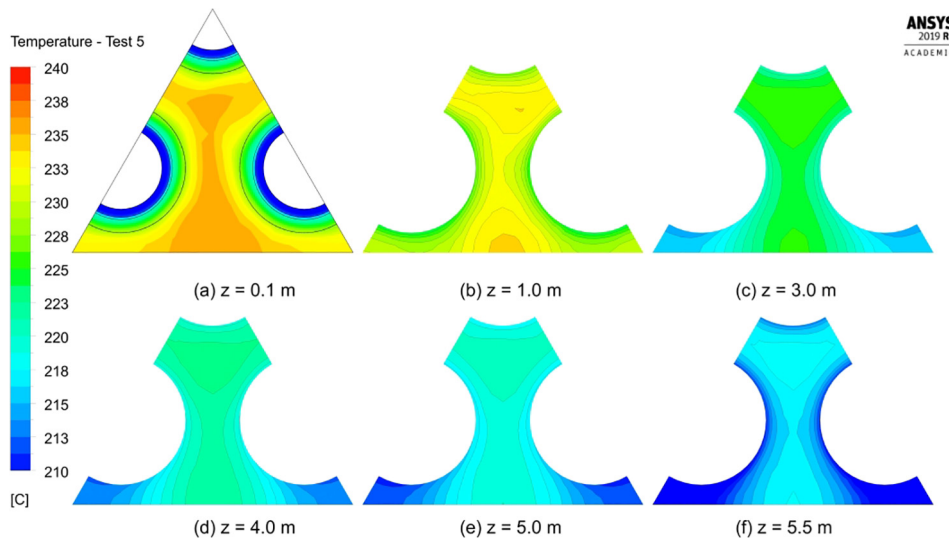

Fig. 16. Coupled simulations – Temperature distribution at different heights in Test 5.
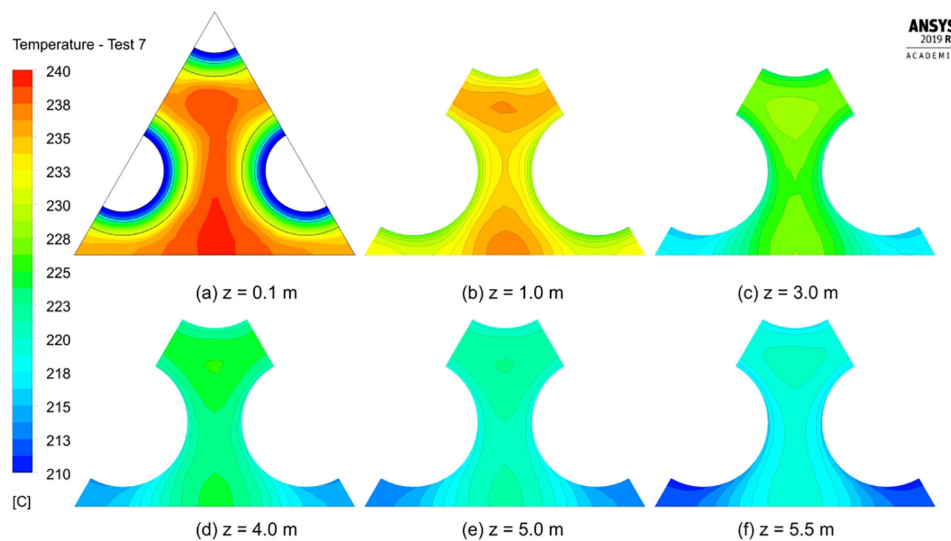
Fig. 17. Coupled simulations – Temperature distribution at different heights – Test 7.

difference is located at the bottom of the primary side (5.5 m in the plots) and it is about 2 K and 4 K for the central (TC-01) and lateral channels (TC-07) respectively. A larger error is found comparing the computed results for the temperature near the wall (thermocouples TC-W0, TC-W1 and TC-W2), with the largest discrepancies located toward the initial section of the evaporator; the maximum variance is about 4 K and it is found at the first axial location (~1.4 m) for Test 5.

Several reasons might be the cause of these differences between calculated and experimental temperatures. In particular, the known difficulties in predicting flow conditions involving two-phase flows must be highlighted as they may play an important role in the definition of the observed discrepancies. In fact, the heat transfer correlations implemented in STH codes relevantly depend on the predicted flow conditions and even small changes may imply large variation in the predicted heat transfer coefficient. The observed temperature reduction at the bottom of the steam generator may be due to the overestimation of the heat transfer coefficient at the beginning of the rising part of the bayonet tube, were boiling is at its onset.

In addition, the simulated geometry does not perfectly match the real one: assuming perfect periodic conditions inside the evaporator (i.e. splitting the geometry into six equal parts) and neglecting the effects of the rod separators could influence the numerical results. Eventually, the properties of the involved materials adopted in the simulations may not perfectly match the real ones; this is a point that might need further investigation and will be considered in future works.

Nonetheless, it should be pointed out that the major causes of uncertainties remain on the experimental side: the measurements of the thermocouples close to the rod separators and to the wall tubes are highly likely to be influenced by local effects on the flow, due to the channels of the separators and the size of the thermocouples themselves.

Therefore, it is important to remark that the numerical results provide a good estimate of the experimental data.

4.2. Temperature – cross section distribution

The main advantage of using CFD calculation is the possibility to analyse the cross-section distribution of the LBE variables inside the primary side. This feature can help highlight the flaws in the design of the heat exchanger and improve the evaluation of the overall efficiency with a considerably deeper insight than that provided by the STH codes alone.

The computed temperature distributions at several cross sections, placed at different heights, for 5 test cases are shown in figures from 13

to 16. For the sake of clarity, the sub-figure (a) includes also the temperature of the solid parts of the pipes and their boundaries, which are marked by a continuous black line.

All the cases show essentially the same behaviour: the highest temperature is first seen in the region close to the wrapper wall, since it is where the LBE inlet is placed (Fig. 13(a) and (b)); then, further down, the temperature becomes higher in the region close to the central pipe (Fig. 13(e) and (f)).

It is possible to see that the temperature distribution around the lateral pipe is noticeably lower than that close to the central pipe, particularly when considering the side facing the wrapper wall. This effect increases towards the bottom of the pipe and it is likely due to the small flow-through section between the lateral pipes and the wrapper walls. As a consequence of this fact, the power to flow area ratio of the lateral subchannels becomes larger than the one faced by the central subchannel, coherently resulting in lower temperature distribution.

5. Conclusions

This work was focused on the coupled simulations of the HX-HERO steam generator installed in the CIRCE–HERO facility. To this end, the CFD-STH coupling model developed at the University of Pisa for the analysis of the CIRCE–HERO facility was improved in order to take into account the application to thermal boundary conditions.

The coupling technique was applied to the whole HX-HERO test section: the pipe structures and the primary (LBE) side were simulated with the CFD code Ansys Fluent whilst the secondary side (water/vapour) was modelled with the one-dimensional STH code RELAP5/Mod3.3. The coupling methodology was tested against the experimental data provided by ENEA at the end of their experimental campaign. A total of nine different test cases were simulated and the predicted temperatures were compared with the experimental ones, both for the primary and the secondary side. The comparison found a general underprediction of the temperature distributions LBE side when compared with the experimental results; this discrepancy might be due to several reasons such as the incorrect estimation of two-phase side convective heat transfer coefficient, of the properties of the material composing the bayonet tubes or simplifying assumptions of the computational geometry; in particular, the thermal conductivity of the AISI316 powder mixed with the Helium gas still retains some degrees of uncertainty and might need further investigation. However, given the uncertainties of the experimental measurements, the error can be considered small.

Nevertheless, the numerical results captured properly the axial trend of the temperatures and provided an overall good prediction also

from a quantitative point of view, particularly for the secondary side, where the experimental trend was correctly reproduced by the coupled simulations. It is important to notice as well that this good performance remained consistent for all the cases, proving the general applicability of the methodology.

The coupled code application, comparing to a standalone STH calculation, may also offer more detailed results thanks to the CFD side; in particular, in the present paper the cross-sectional distributions of the LBE temperature were investigated for different axial positions. The analysis highlighted the presence of a colder region of fluid in the regions close to the external wall. This phenomenon is likely due to the different thermal load faced by the subchannels in which the bundle may be ideally subdivided.

CRediT authorship contribution statement

F. Galleni: Methodology, Investigation, Writing - original draft, Writing - review & editing. **G. Barone:** Methodology, Writing - review & editing. **D. Martelli:** Methodology, Writing - review & editing. **A. Pucciarelli:** Writing - review & editing. **P. Lorusso:** Writing - review & editing. **M. Tarantino:** Writing - review & editing. **N. Forgione:** Supervision, Writing - review & editing.

Declaration of Competing Interest

The authors declare that they have no known competing financial interests or personal relationships that could have appeared to influence the work reported in this paper.

Acknowledgments

References

Ambrosini, W., Azzati, M., Benamati, G., Bertacci, G., Cinotti, L., Forgione, N., Oriolo, F., Scaddozzo, G., Tarantino, M., 2004. Testing and qualification of CIRCE instrumentation based on bubble tubes. Journal of Nuclear Materials, Proceedings of the 3rd International Workshop on Materials for Hybrid Reactors and Related Technologies 335, 293–298. doi: 10.1016/j.jnucmat.2004.07.030.

Angelucci, M., Martelli, D., Barone, G., Di Piazza, I., Forgione, N., 2017. STH-CFD codes coupled calculations applied to HLM loop and pool systems. Sci. Technol. Nucl. Installations 2017, 1–13. https://doi.org/10.1155/2017/1936894.

Angelucci, M., Martelli, D., Forgione, N., Tarantino, M., 2017b. RELAP5 STH and Fluent CFD Coupled Calculations of a PLOHS + LOF Transient in the HLM Experimental Facility CIRCE V008T09A045. doi: 10.1115/ICONE25-67278.

ANSYS Inc., 2018. ANSYS Fluent User's Guide, Release 19.2.

Baeten, P., 2015. MYRTE Deliverable 1.3 – Dissemination and communication action plan (No. SCK•CEN/6426174). SCK•CEN.

Benamati, G., Foletti, C., Forgione, N., Oriolo, F., Scaddozzo, G., Tarantino, M., 2007. Experimental study on gas-injection enhanced circulation performed with the CIRCE facility. Nucl. Eng. Des. 237, 768–777. https://doi.org/10.1016/j.nucengdes.2006.09.005.

Buzzi, F., Pucciarelli, A., Galleni, F., Tarantino, M., Forgione, N., 2020. Analysis of thermal stratification phenomena in the CIRCE-HERO facility. Ann. Nucl. Energy 141, 107320. https://doi.org/10.1016/j.anucene.2020.107320.

Fazio, C. (Ed.), 2015. Handbook on Lead-bismuth Eutectic Alloy and Lead Properties, Materials Compatibility, Thermal-hydraulics and Technologies – 2015 Edition (No. NEA–7268). Organisation for Economic Co-Operation and Development.

Forgione, N., Angelucci, M., Ulissi, C., Martelli, D., Barone, G., Ciolini, R., Tarantino, M., 2019. Application of RELAP5/Mod3.3 – fluent coupling codes to CIRCE-HERO. J. Phys. Conf. Ser. 1224, 012032. https://doi.org/10.1088/1742-6596/1224/1/012032.

Lorusso, P., Pesetti, A., Barone, G., Castelliti, D., Caruso, G., Forgione, N., Giannetti, F., Martelli, D., Rozzia, D., Van Tichelen, K., Tarantino, M., 2019. MYRRHA primary heat exchanger experimental simulations on CIRCE-HERO. Nucl. Eng. Des. 353. https://doi.org/10.1016/j.nucengdes.2019.110270.

Lorusso, P., Pesetti, A., Tarantino, M., 2018. Alfred steam generator assessment: Design and pre-test analysis of hero experiment. Presented at the International Conference on Nuclear Engineering, Proceedings, ICONE. doi: 10.1115/ICONE26-81824.

Lorusso, P., Pesetti, A., Tarantino, M., Narcisi, V., Giannetti, F., Forgione, N., Del Nevo, A., 2019. Experimental analysis of stationary and transient scenarios of alfred steam generator bayonet tube in circe-hero facility. Nucl. Eng. Des. 352, 110169. https://doi.org/10.1016/j.nucengdes.2019.110169.

Lorusso, P., Pesetti, A., Tarantino, M., Polazzi, G., Sermenghi, V., 2018. CIRCE Experimental report (No. CI-I-R-353), D3.2 – MYRTE. ENEA.

Martelli, D., Forgione, N., Barone, G., di Piazza, I., 2017. Coupled simulations of the NACIE facility using RELAP5 and ANSYS FLUENT codes. Ann. Nucl. Energy 101, 408–418. https://doi.org/10.1016/j.anucene.2016.11.041.

Martelli, D., Marinari, R., Barone, G., di Piazza, I., Tarantino, M., 2017. CFD thermo-hydraulic analysis of the CIRCE fuel bundle. Ann. Nucl. Energy 103, 294–305. https://doi.org/10.1016/j.anucene.2017.01.031.

MYRTE Project (No. Grant Agreement N. 662186), 2015. . EURATOM H2020.

Narcisi, V., Giannetti, F., Tarantino, M., Martelli, D., Caruso, G., 2017. Pool temperature stratification analysis in CIRCE-ICE facility with RELAP5-3D© model and comparison with experimental tests. J. Phys.: Conf. Ser. 923, 012006. https://doi.org/10.1088/1742-6596/923/1/012006.

Nuclear Safety Analysis Division, 2001. RELAP5/MOD3.3 Code Manual Volumes 1-8. Information Systems Laboratories, Inc., Rockville, Maryland, Idaho Falls, Idaho.

Pesetti, A., Forgione, N., Narcisi, V., Lorusso, P., Giannetti, F., Tarantino, M., Del Nevo, A., 2018. ENEA CIRCE-HERO TEST FACILITY: GEOMETRY AND INSTRUMENTATION DESCRIPTION (No. CI-I-R-343), H2020 SESAME Project. ENEA.

Pucciarelli, A., Barone, G., Forgione, N., Galleni, F., Martelli, D., 2020. NACIE-UP post-test simulations by CFD codes. Nucl. Eng. Des. 356, 110392. https://doi.org/10.1016/j.nucengdes.2019.110392.

Roelofs, F., Shams, A., Pacio, J., Moreau, V., Planquart, P., van Tichelen, K., Piazza, I.D., Tarantino, M., 2015. European Outlook for LMFR Thermal Hydraulics, in: The 16th International Topical Meeting on Nuclear Reactor Thermal Hydraulics (NURETH-16), Chicago, United States. Presented at the NURETH-16, p. 12.

Shams, A., Roelofs, F., Baglietto, E., Lardeau, S., Kenjeres, S., 2014. Assessment and calibration of an algebraic turbulent heat flux model for low-Prandtl fluids. Int. J. Heat Mass Transf. 79, 589–601. https://doi.org/10.1016/j.ijheatmasstransfer.2014.08.018.